

Electronic Supplementary Information (ESI)

**Microporous carbons derived from nitrogen-rich triazatruxene-based
porous organic polymers for efficient cathodic supercapacitors**

Ahmed F. Saber, Shiao-Wei Kuo, and Ahmed F. M. EL-Mahdy*

Department of Materials and Optoelectronic Science, National Sun Yat-Sen University,
Kaohsiung 80424, Taiwan

*To whom correspondence should be addressed

E-mail: ahmedelmahdy@mail.nsysu.edu.tw

Section	Content	Page No.
S1	Materials	S3
S2	Characterization	S3
S3	Synthetic Procedures of Monomers	S4
S4	Synthetic Procedures of CMPs	S9
S5	FTIR and NMR Spectral Profiles of Monomers	S11
S6	FTIR Spectral Profiles of CMPs	S16
S7	Thermal Gravimetric Analysis	S17
S8	X-ray Photoelectron Spectroscopy Analysis	S18
S9	The Proposed Chemical Structure of Carbon Materials	S20
S10	X-ray Diffraction Analysis	S21
S11	Raman Spectroscopy	S21
S12	Elemental Analysis	S22
S13	Surface Area Parameters	S22
S14	Low Magnification HR-TEM Spectroscopy	S23
S15	Contact Angle	S23
S16	Electrochemical Methods and Data	S23
S17	References	S28

S1. Materials

All solvents and chemicals were obtained from commercial suppliers and used as received unless otherwise noted. Carbazole, potassium acetate, sodium carbonate, sodium sulphate (Na_2SO_4), potassium hydroxide (KOH), potassium permanganate (KMnO_4), ethyl iodide ($\text{C}_2\text{H}_5\text{I}$), phosphorus oxychloride (POCl_3), hexane, 1,1'-bis(diphenylphosphino)ferrocene] dichloropalladium (II), bis(pinacolato)diboron (99%) were ordered from Sigma-Aldrich. Tetrakis(triphenylphosphine)palladium (0) (99%) was purchased from Acros. Dimethylformamide (DMF), dichloromethane (DCM) and dioxane were obtained from J. T. Baker. Tetrahydrofuran (THF, 99.9%) was ordered from Showa (Tokyo, Japan). Whereas *N*-bromosuccinimide (NBS, 99%), anhydrous magnesium sulfate (MgSO_4 , 99.5%), potassium carbonate (K_2CO_3 , 99.9%) and methanol (MeOH), and acetone were ordered from Alfa Aesar. Ethyl acetate was obtained from ECHO chemical co. LTD.

S2. Characterizations

Fourier-transform infrared spectroscopy (FTIR). FTIR spectra were recorded using a Bruker Tensor 27 FTIR spectrophotometer and the conventional KBr plate method; 32 scans were collected at a resolution of 4 cm^{-1} .

Solid state nuclear magnetic resonance (SSNMR) spectroscopy. SSNMR spectra were recorded using a Bruker Avance 400 NMR spectrometer and a Bruker magic-angle-spinning (MAS) probe, running 32,000 scans.

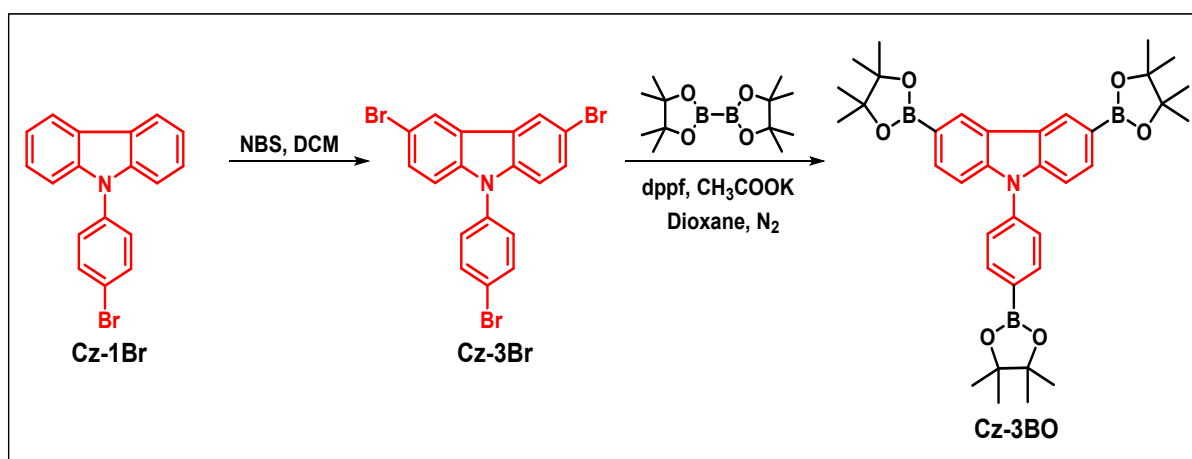
Thermogravimetric analysis (TGA). TGA was performed using a TA Q-50 analyzer under a flow of N_2 . The samples were sealed in a Pt cell and heated from 40 to 800 °C at a heating rate of 20 °C min^{-1} under N_2 at a flow rate of 50 mL min^{-1} .

Surface area and porosimetry (ASAP/BET). The BET surface areas and porosimetry investigations of the prepared samples (ca. 20–100 mg) were conducted using a Micromeritics ASAP 2020 Surface Area and Porosity analyzer. Nitrogen isotherms were generated through incremental exposure to ultrahigh-purity N₂ (up to ca. 1 atm) in a liquid N₂ (77 K) bath.

Field-emission scanning electron microscopy (FE-SEM). FE-SEM was performed using a JEOL JSM-7610F scanning electron microscope. Samples were subjected to Pt sputtering for 100 s prior to observation.

Transmission electron microscopy (TEM). TEM was accomplished using a JEOL-2100 scanning electron microscope, operated at 200 kV.

S3. Synthetic Procedures of Monomers



Scheme S1. Synthesis of 3,6-bis(4,4,5,5-tetramethyl-1,3,2-dioxaborolan-2-yl)-9-(4-(4,4,5,5-tetramethyl-1,3,2-dioxaborolan-2-yl)phenyl)-9H-carbazole (Cz-3BO).

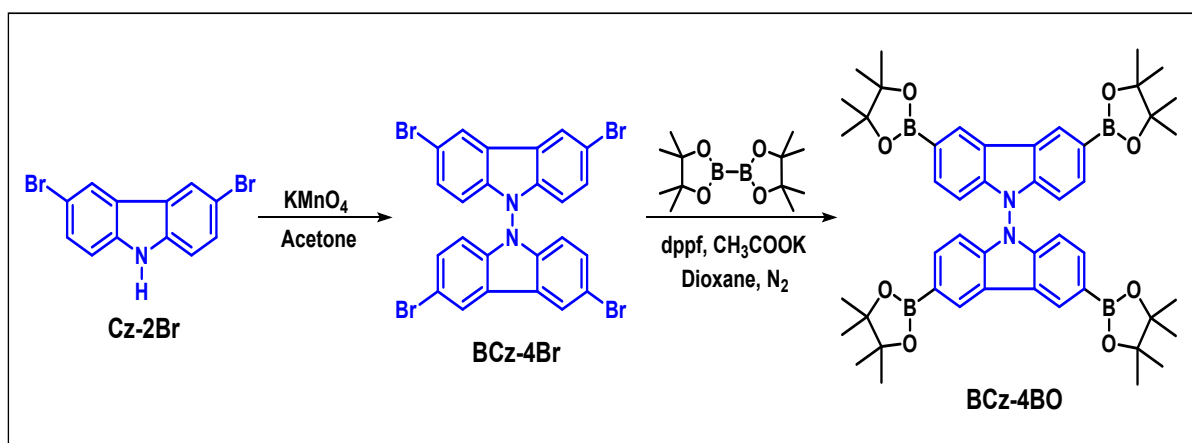
Synthesis of 3,6-dibromo-9-(4-bromophenyl)-9H-carbazole (Cz-3Br): [S1]

9-(4-bromophenyl)-9H-carbazole (1.0 g, 3.10 mmol) was dissolved in DCM (17 mL) in a Schlenk flask wrapped with aluminum foil. NBS (1.36 g, 7.69 mmol) was added as solid at 0°C in the dark and the reaction mixture was stirred overnight (~16 h). It was quenched with water and extracted with dichloromethane (3 x 40 mL). The combined organic extracts were dried over anhydrous MgSO₄ and filtered. The organic layer evaporated under reduced

pressure. The residue was purified by silica gel chromatography with hexanes as the eluent to afford tribromo carbazole as a crystalline solid. Yield: 1.46 g (98%). m.p. 208-210°C. ¹H NMR (400 MHz, CDCl₃) δ (ppm): 7.21 (d, 2H), 7.38 (d, 2H), 7.50 (dd, 2H), 7.74 (d, 2H), 8.18 (d, 2H). ¹³C NMR (100 MHz, CDCl₃) δ (ppm): 111.46, 113.54, 121.90, 123.51, 124.21, 128.72, 129.74, 133.57, 136.00, 139.77.

Synthesis of 3,6-bis(4,4,5,5-tetramethyl-1,3,2-dioxaborolan-2-yl)-9-(4-(4,4,5,5-tetramethyl-1,3,2-dioxaborolan-2-yl)phenyl)-9H-carbazole (Cz-3BO): [S2]

In a dried and cleaned 100 mL two neck-bottle, a mix of 3,6-dibromo-9-(4-bromophenyl)-9H-carbazole (Cz-3Br) (1.2 g, 2.5 mmol), bis(pinacolato)diboron (2.1 g, 8.27 mmol), potassium acetate (0.74 g, 7.54 mmol), and 1,1'-bis(diphenylphosphino)ferrocene]dichloropalladium (II) (0.12 g, 0.16 mmol) in *p*-dioxane (15 mL) was heated at 110°C under nitrogen atmosphere for 2 days. Then, the reaction mixture was allowed to cool to room temperature, to be poured into iced-water. The formed precipitate was collected by extraction with dichloromethane and dried under vacuum overnight. The residue was purified by flash chromatographically (SiO₂; THF/Hexane = 1:4) to provide a white solid (1.0 g, 65.5%). FTIR (KBr, cm⁻¹): 3045, 2981, 2928, 1606, 1350. ¹H NMR (500 MHz, CDCl₃) δ (ppm): 7.25-8.69 (m, 10H), 1.40 (s, 36H). ¹³C NMR (125 MHz, CDCl₃) δ (ppm): 143.64, 137.03, 127.31, 84.09, 24.91.



Scheme S2. Synthesis of 3,3',6,6'-tetraboronic-pinacolate-9,9'-bicarbazole (BCz-4BO).

Synthesis of 3,6-Dibromocarbazole (Cz-2Br): [S3]

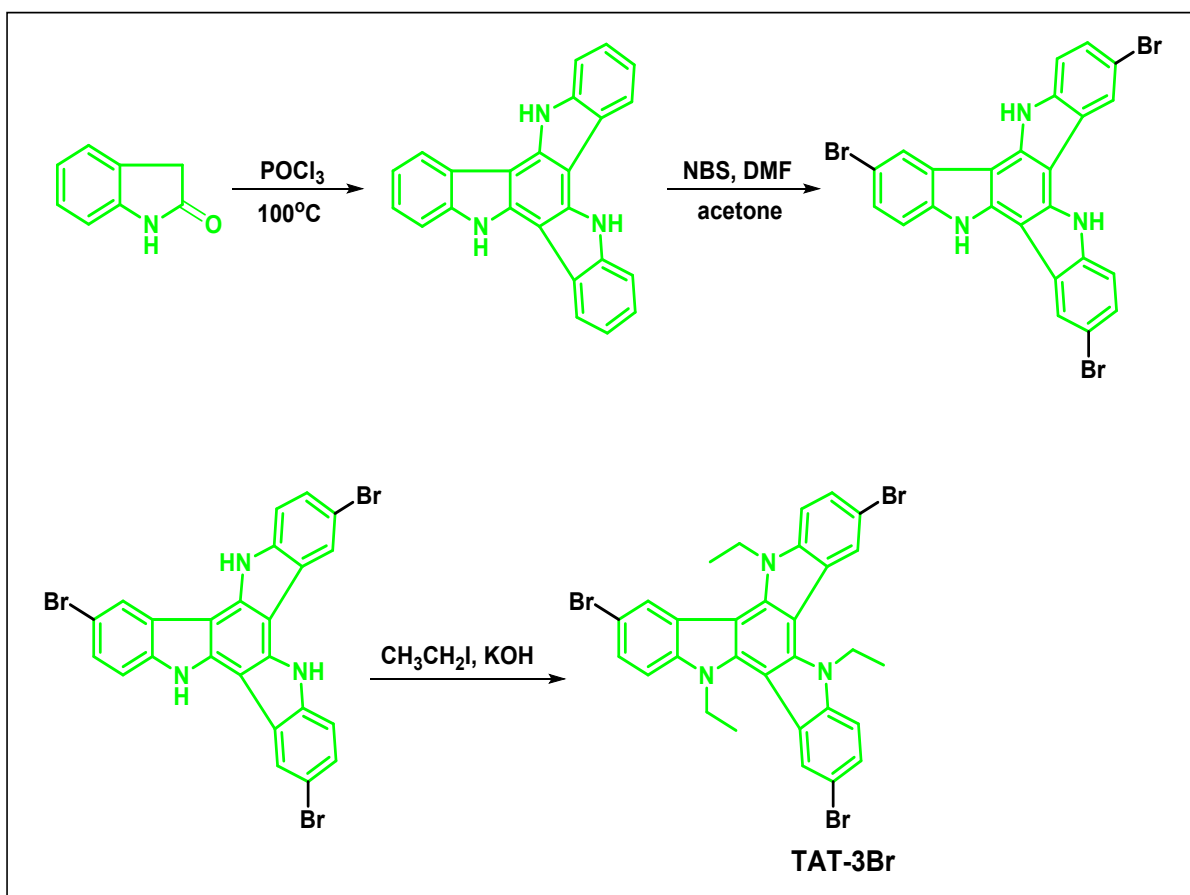
A solution of NBS (10.7 g, 60.0 mmol) in DMF (50 mL) was added slowly to a suspension of carbazole (5.00 g, 30.0 mmol) in DCM (300 mL). The mixture was stirred at room temperature overnight. The solution was washed with water (3 x 150 mL); the organic phase was separated, and the solvent was evaporated. The solid residue was washed with DCM, then dried under vacuum to yield Cz-2Br (7.7 g, 82%). ¹H NMR (500 MHz, DMSO) δ (ppm): 11.58 (br, 1H, NH), 8.41 (s, 2H), 7.52 (d, 2 H), 7.42 (d, 2H). ¹³C NMR (125 MHz, DMSO) δ (ppm): 139.42, 129.42, 124.34, 123.47, 112.97, 112.32.

Synthesis of 3,3',6,6'-tetrabromo-9,9'-bicarbazole (BCz-4Br): [S3]

KMnO₄ (2.92 g, 90.0 mmol) was added to a solution of Cz-2Br (2.00 g, 30.0 mmol) in acetone (40 mL) at 50°C. The solution was then hydrolyzed through the addition of distilled water (100 mL). The mixture was extracted with DCM and the solvent evaporated. The residue was washed with MeOH to yield CB-4Br (6.92 g, 71%). ¹H NMR (500 MHz, CDCl₃) δ (ppm): 8.27 (d, 4H), 7.47 (dd, 4H), 6.75 (d, 4H). ¹³C NMR (125 MHz, CDCl₃) δ (ppm): 139.31, 131.19, 124.81, 123.30, 115.41, 110.59.

Synthesis of 3,3',6,6'-tetraboronic-pinacolate-9,9'-bicarbazole (BCz-4BO): [S4]

A mixture of BC-4Br (1.87g, 2.90 mmol), bis(pinacolate)diboron (4.4 g, 17.35 mmol), [1,1'-bis(diphenylphosphino)ferrocene] dichloropalladium(II) (183 mg, 0.25 mmol) and potassium acetate (1.75 g, 17.85 mmol) were heated at reflux in dioxane at 100°C for two days under N₂ atmosphere. The solution was poured into a stirred beaker filled with ice cubes and H₂O. The product was extracted with DCM then purified chromatographically through (SiO₂; hexane/EtOAc, 3:1) to give BC-4BO as a white precipitate (2.18 g, yield, 90%). FTIR (KBr, cm⁻¹): 2977, 2929, 2862, 1602, 1345, 1456, 1148, 1080. ¹H NMR (500 MHz, CDCl₃) δ (ppm): 8.70 (s, 4H), 7.71 (d, 4H), 6.80 (d, 4H), 1.32 (s, 48H). ¹³C NMR (125 MHz, CDCl₃) δ (ppm): 141.65, 133.11, 128.58, 121.58, 108.12, 88.47, 24.16.



Scheme S3. Synthesis of 3,8,13-tribromo-5,10,15-triethyl-10,15-dihydro-5H-diindolo[3,2-a:3',2'-c]carbazole (TAT-3Br).

Synthesis of 10,15-dihydro-5H-diindolo[3,2-a:3',2'-c] carbazole (TAT): [S5]

Prepared with a slight modification to what was published in literature. Under nitrogen atmosphere, a mixture of 2-indolinone (10 g, 75 mmol) and POCl_3 (50 mL) was heated at 100°C for 8h. Then, the reaction mixture was poured into ice and neutralized carefully with Na_2CO_3 . After neutralization, the precipitate was filtered to give the crude product as a brown solid. The crude solution in MeOH was absorbed on silica-gel, dried, loaded and eluted through a thick silica-gel pad with a DCM as a mobile phase. After evaporation of eluate at reduced pressure and recrystallization from acetone, pure pale-yellow solid was obtained (5.5 g, 63%). ^1H NMR (400 MHz, DMSO) δ (ppm): 11.86 (s, 3H), 8.66 (d, 3H), 7.71 (d, 3H), 7.41-7.28 (m, 6H). ^{13}C NMR (100 MHz, Acetone) δ (ppm): 141.0, 136.4, 124.8, 124.5, 121.5, 121.4, 112.9, 103.3.

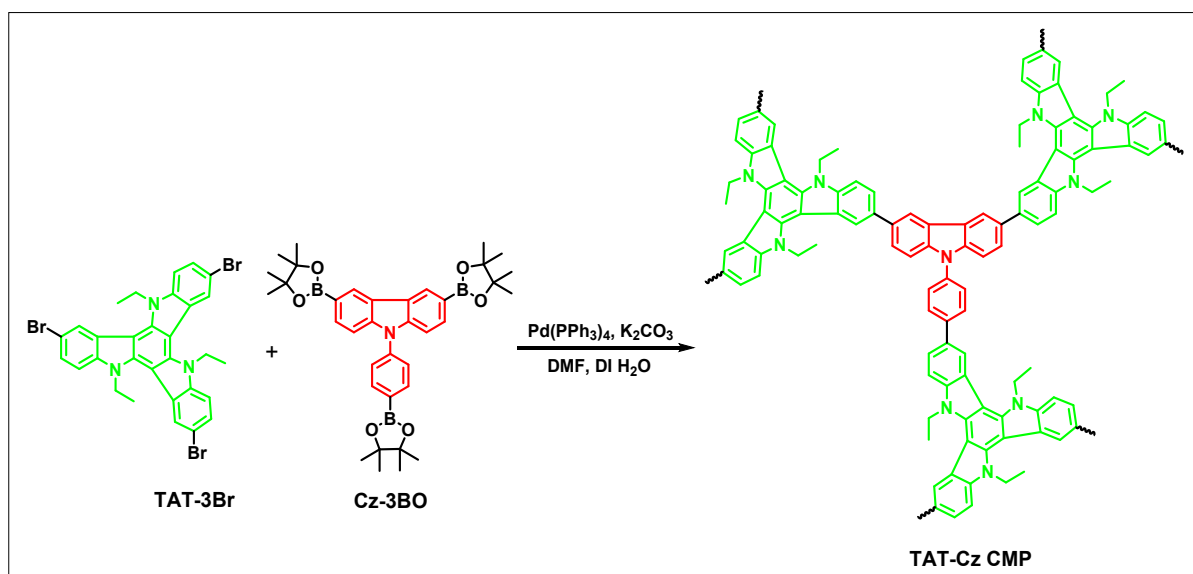
Synthesis of 3,8,13-tribromo-10,15-dihydro-5*H*-diindolo[3,2-*a*:3',2'-*c*]carbazole: [S6]

A solution of NBS (0.28 g, 1.55 mmol) in DMF (2 mL) was added dropwise to a mixture of triindole (0.17 g, 0.5 mmol) in acetone (10 mL) at 0°C. The mixture was slowly warmed to room temperature and stirred for an additional 30 min before it was poured into water. Then, the organic phase was separated and dried over anhydrous Na₂SO₄. After the solvent was evaporated, the crude product was purified by column chromatography using hexane/acetone (8:2) as the eluent to afford triindole-3Br as a pale white solid (0.22 g, 76%). ¹H NMR (400 MHz, acetone) δ (ppm): 11.34 (s, 3H), 8.39 (d, 3H), 7.85 (s, 3H), 7.45 (d, 3H).

Synthesis of 3,8,13-tribromo-5,10,15-triethyl-10,15-dihydro-5*H*-diindolo[3,2-*a*:3',2'-*c*]carbazole (TAT-3Br):

A mixture of triindole-3Br (0.15 g, 0.25 mmol) and KOH (0.28 g, 5 mmol) was stirred at room temperature, then a solution of ethyl iodide (0.12 mL, 1.5 mmol) was added slowly, the mixture was stirred overnight. The mixture was poured into water and extracted with EtOAc. The combined organic layer was dried over anhydrous Na₂SO₄, filtered, and concentrated under reduced pressure. The crude product was purified by chromatography (EtOAc: hexane, 5:95) to give the triethyl derivative as a yellow solid (0.22 g, 95%). FTIR (KBr, cm⁻¹): 2955, 2923, 1565, 795. ¹H NMR (400 MHz, CDCl₃) δ (ppm): 1.55 (t, 3H), 4.84 (q, 2H), 7.45-8.06 (m, 9H). ¹³C NMR (100 MHz, CDCl₃) δ (ppm): 142.33, 139.14, 126.08, 122.65, 117.33, 113.86, 103.57, 102.58, 41.90, 15.46.

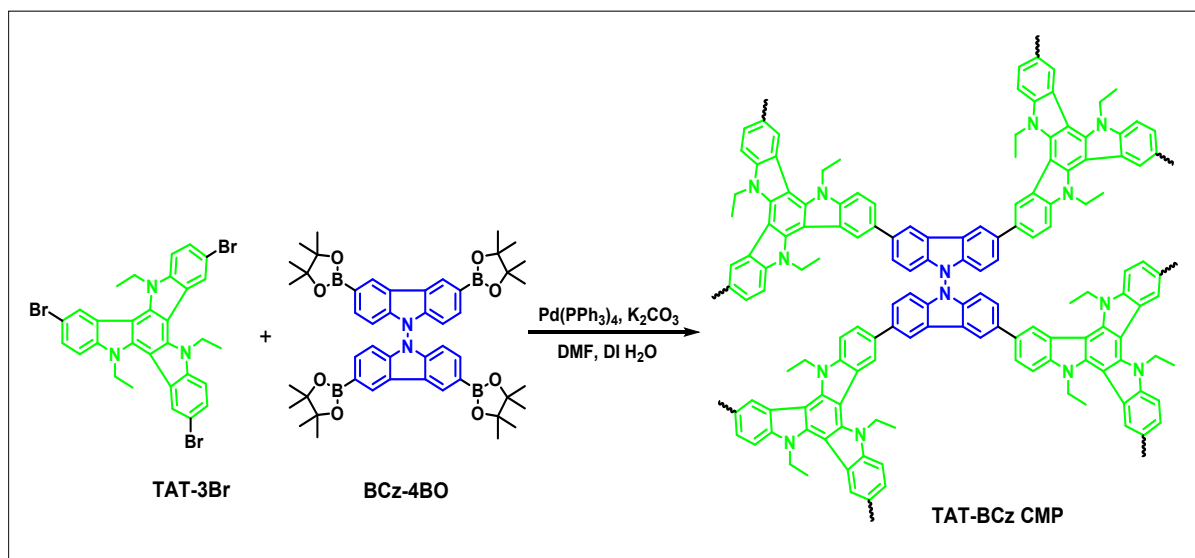
S4. Synthetic Procedures of CMPs



Scheme S4. Synthesis of TAT-Cz CMP.

Synthesis of TAT-Cz CMP.

In a 25 mL Pyrex tube, a mixture of TAT-3Br (100 mg, 0.15 mmol), Cz-3BO (93.24 mg, 0.15 mmol), tetrakis(triphenylphosphine)palladium (17.34 mg, 0.015 mmol), and potassium carbonate (207.43 mg, 1.50 mmol) was evacuated for 10 mins. Then a co-solvent of DMF and H₂O (5:1, v/v, 12 mL) was added. Degassing of the reaction mixture by freeze–pump–thaw cycles and purging with N₂ was carried out and the closed tube was then stirred at 145°C for 72 hrs. After allowing the mixture to cool at 25°C, the formed precipitate was isolated *via* centrifuging, thoroughly washed sequentially with water, methanol, acetone, and tetrahydrofuran till colorless solution, and extracted by Soxhlet sequentially with methanol and tetrahydrofuran for 72 h. Finally, the obtained precipitate was dried at 120°C for 16 h under vacuum to yield TAT-Cz CMP as a black solid (75.60% yield).



Scheme S5. Synthesis of TAT-BCz CMP.

Synthesis of TAT-BCz CMP.

In a 25 mL Pyrex tube, a mixture of TAT-3Br (100 mg, 0.15 mmol), BCz-4BO (94.14 mg, 0.113 mmol), tetrakis(triphenylphosphine)palladium (17.34 mg, 0.015 mmol), and potassium carbonate (207.43 mg, 1.50 mmol) was evacuated for 10 mins. Then a co-solvent of DMF and H₂O (5:1, v/v, 12 mL) was added. Degassing of the reaction mixture by freeze–pump–thaw cycles and purging with N₂ was carried out and the closed tube was then stirred at 145°C for 72 hrs. After allowing the mixture to cool at 25°C, the formed precipitate was isolated *via* centrifuging, thoroughly washed sequentially with water, methanol, acetone, and tetrahydrofuran till colorless solution, and extracted by Soxhlet sequentially with methanol and tetrahydrofuran for 72 h. Finally, the obtained precipitate was dried at 120°C for 16 h under vacuum to yield TAT-BCz CMP as a black solid (81.35% yield).

S5. FTIR and NMR Spectral Profiles of Monomers

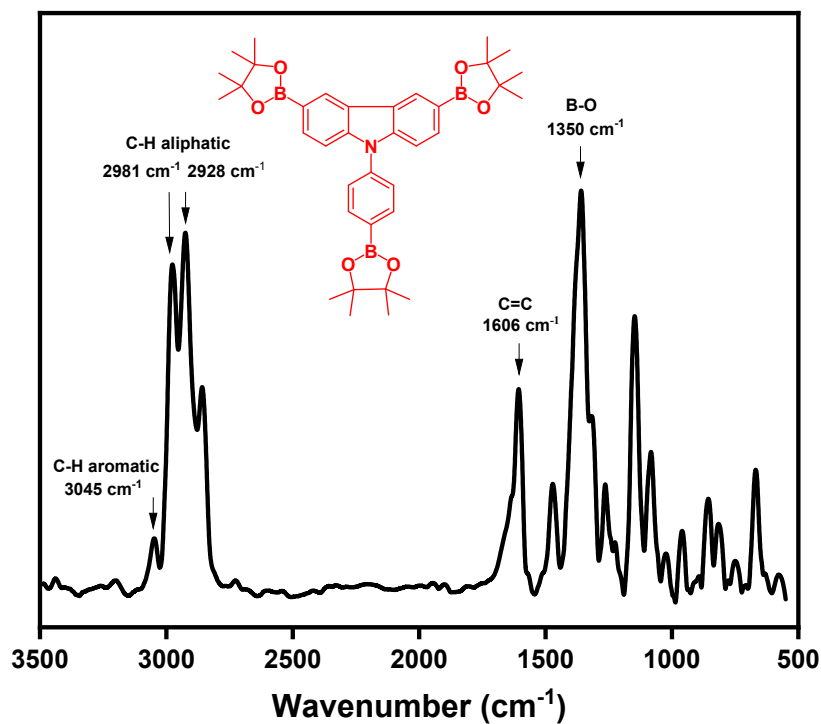


Figure S1. FTIR spectrum of 3,6-bis(4,4,5,5-tetramethyl-1,3,2-dioxaborolan-2-yl)-9-(4-(4,4,5,5-tetramethyl-1,3,2-dioxaborolan-2-yl)phenyl)-9H-carbazole (Cz-3BO).

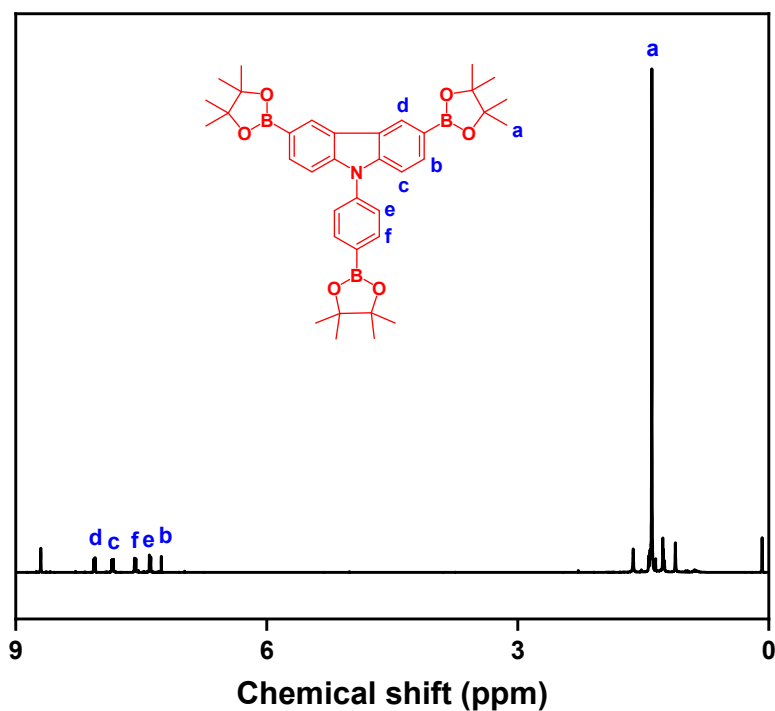


Figure S2. ¹H NMR spectrum of 3,6-bis(4,4,5,5-tetramethyl-1,3,2-dioxaborolan-2-yl)-9-(4-(4,4,5,5-tetramethyl-1,3,2-dioxaborolan-2-yl)phenyl)-9H-carbazole (Cz-3BO).

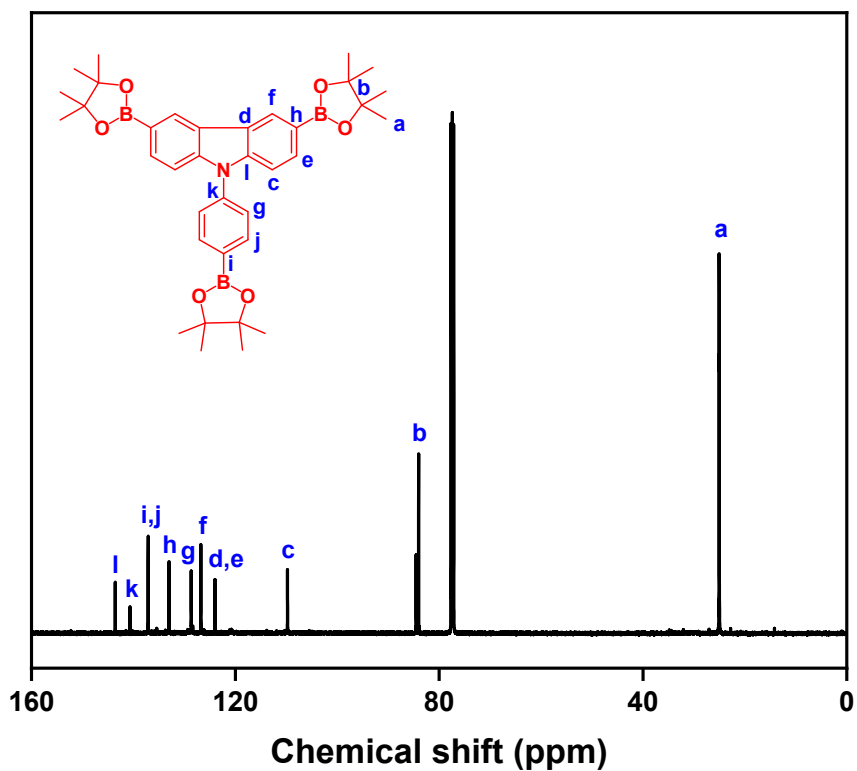


Figure S3. ^{13}C NMR spectrum of 3,6-bis(4,4,5,5-tetramethyl-1,3,2-dioxaborolan-2-yl)-9-(4-(4,4,5,5-tetramethyl-1,3,2-dioxaborolan-2-yl)phenyl)-9H-carbazole (Cz-3BO).

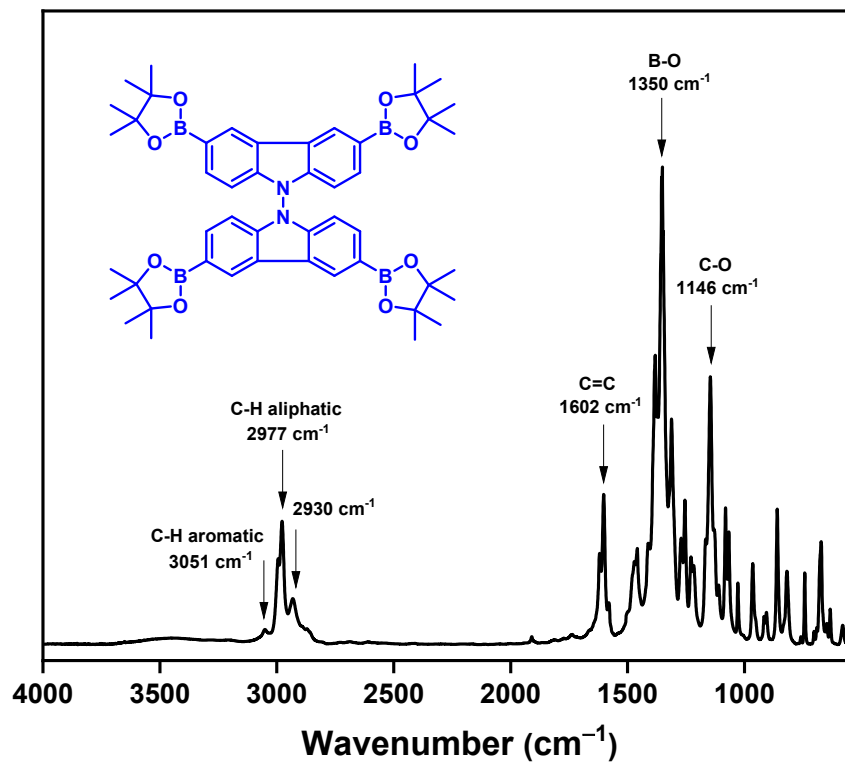


Figure S4. FTIR spectrum of 3,3',6,6'-tetraboronic-pinacolate-9,9'-bicarbazole (BCz-4BO).

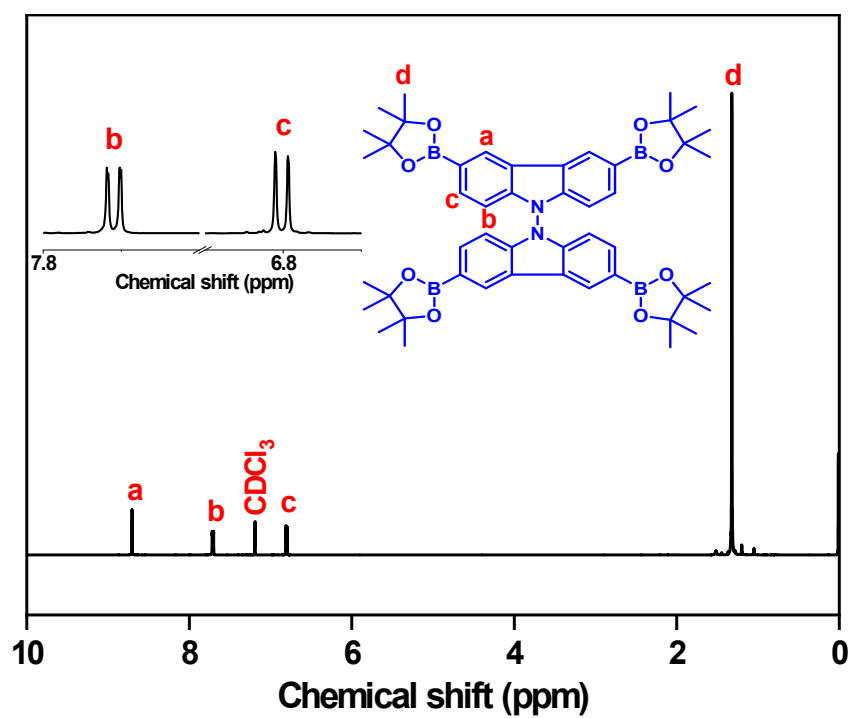


Figure S5. ^1H NMR spectrum of 3,3',6,6'-tetraboronic-pinacolate-9,9'-bicarbazole (BCz-4BO).

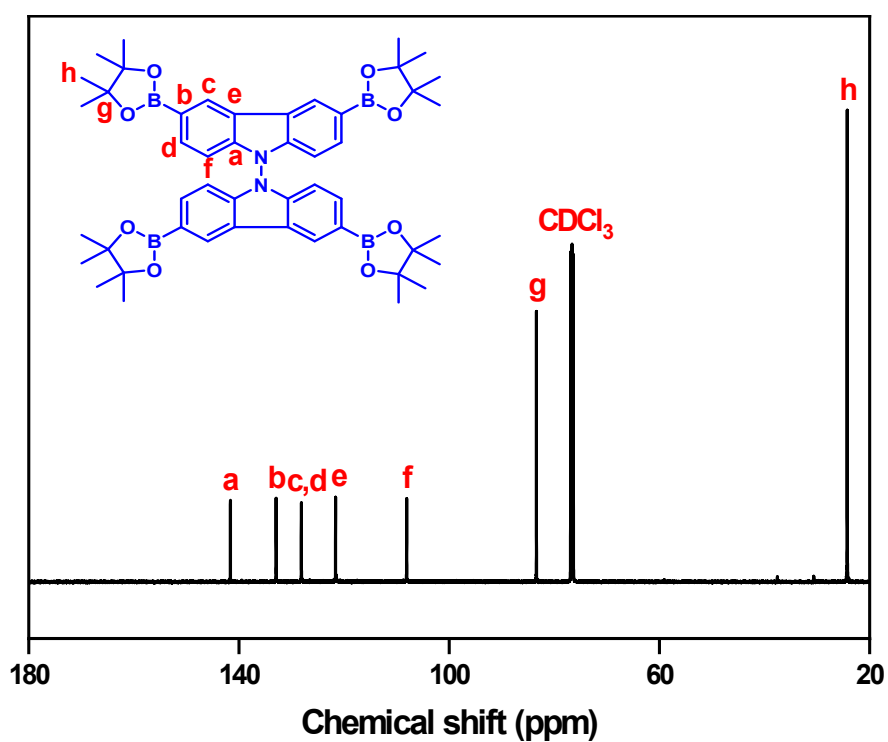


Figure S6. ^{13}C NMR spectrum of 3,3',6,6'-tetraboronic-pinacolate-9,9'-bicarbazole (BCz-4BO).

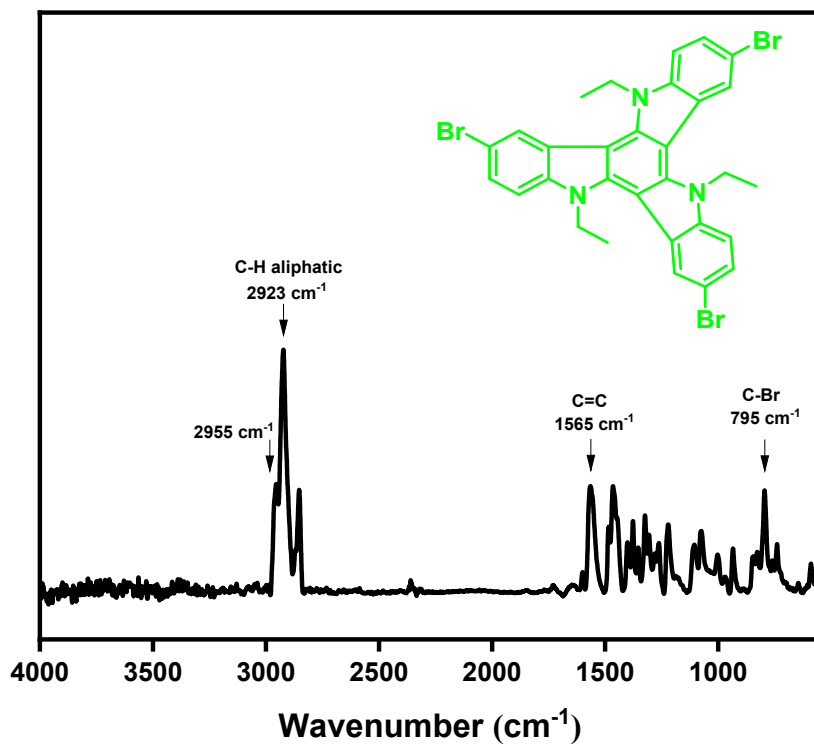


Figure S7. FTIR spectrum of 3,8,13-tribromo-5,10,15-triethyl-10,15-dihydro-5H-diindolo[3,2-a:3',2'-c] carbazole (TAT-3Br).

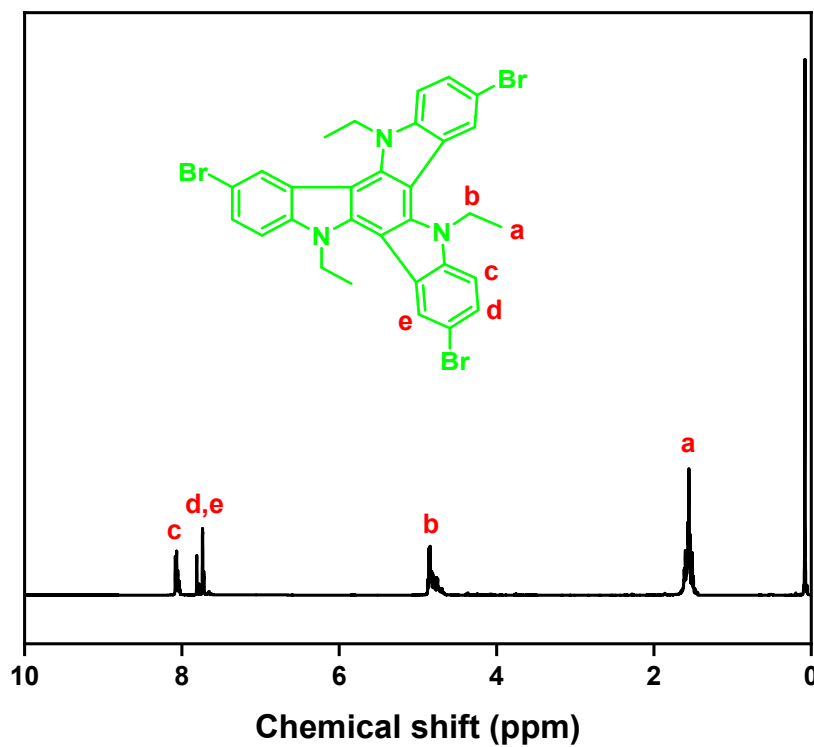


Figure S8. ¹H NMR spectrum of 3,8,13-tribromo-5,10,15-triethyl-10,15-dihydro-5H-diindolo[3,2-a:3',2'-c] carbazole (TAT-3Br).

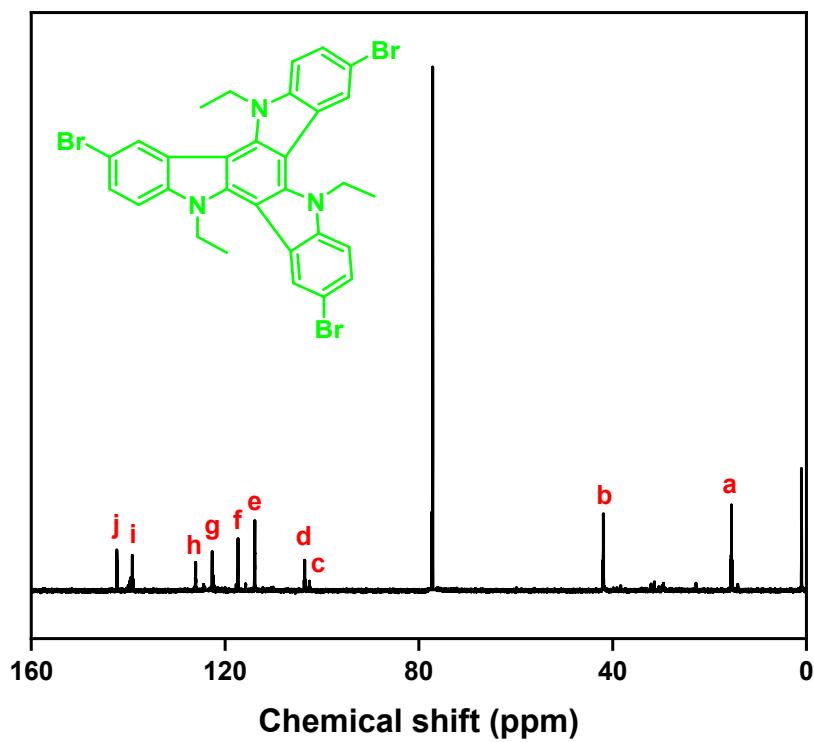


Figure S9. ¹³C NMR spectrum of 3,8,13-tribromo-5,10,15-triethyl-10,15-dihydro-5H-diindolo[3,2-a:3',2'-c] carbazole (TAT-3Br).

S6. FTIR Spectral Profiles of CMPs

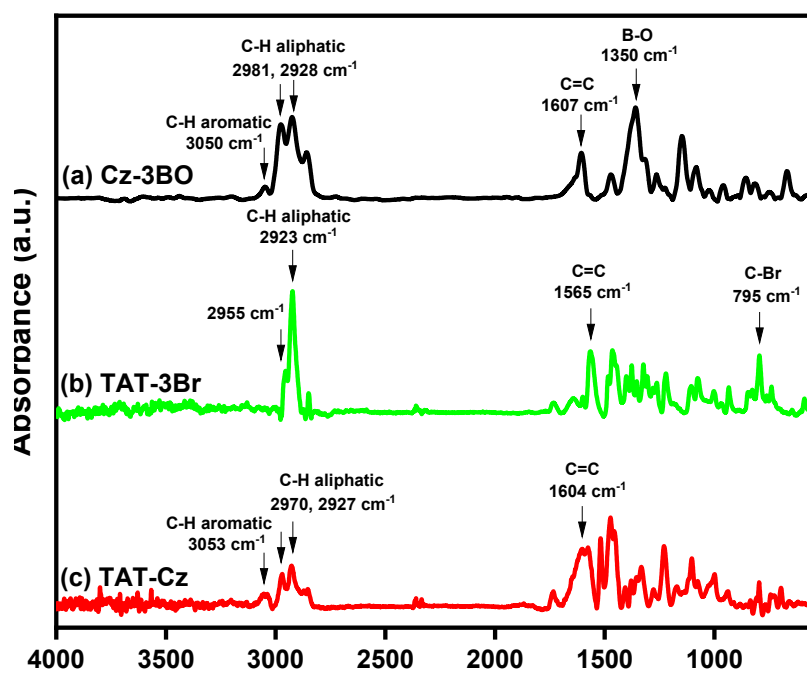


Figure S10. FTIR spectra of (a) Cz-3BO, (b) TAT-3Br, and (c) TAT-Cz CMP.

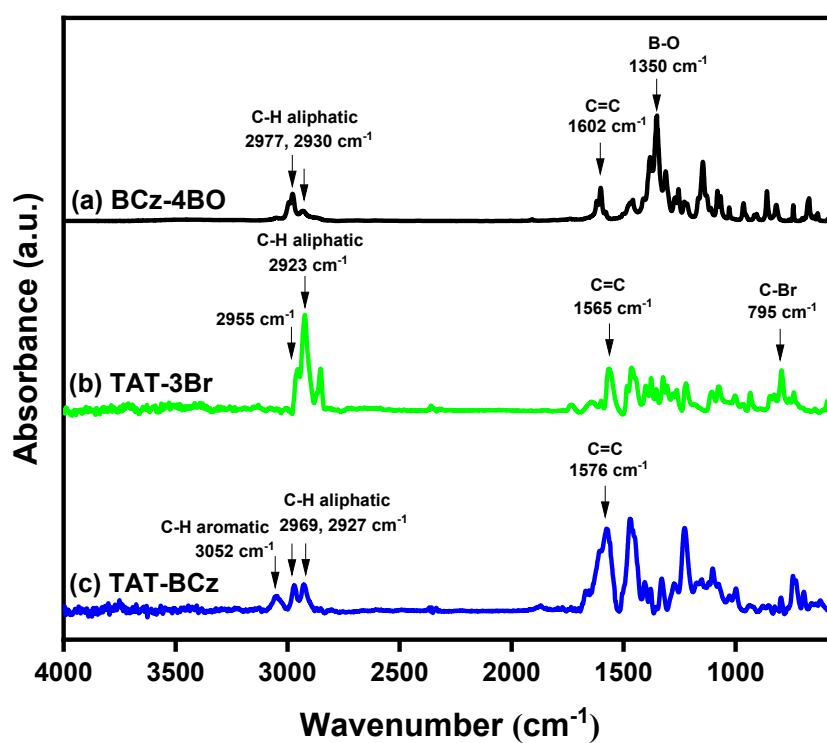


Figure S11. FTIR spectra of (a) BCz-4BO, (b) TAT-3Br, and (c) TAT-BCz CMP.

S7. Thermal Gravimetric Analysis

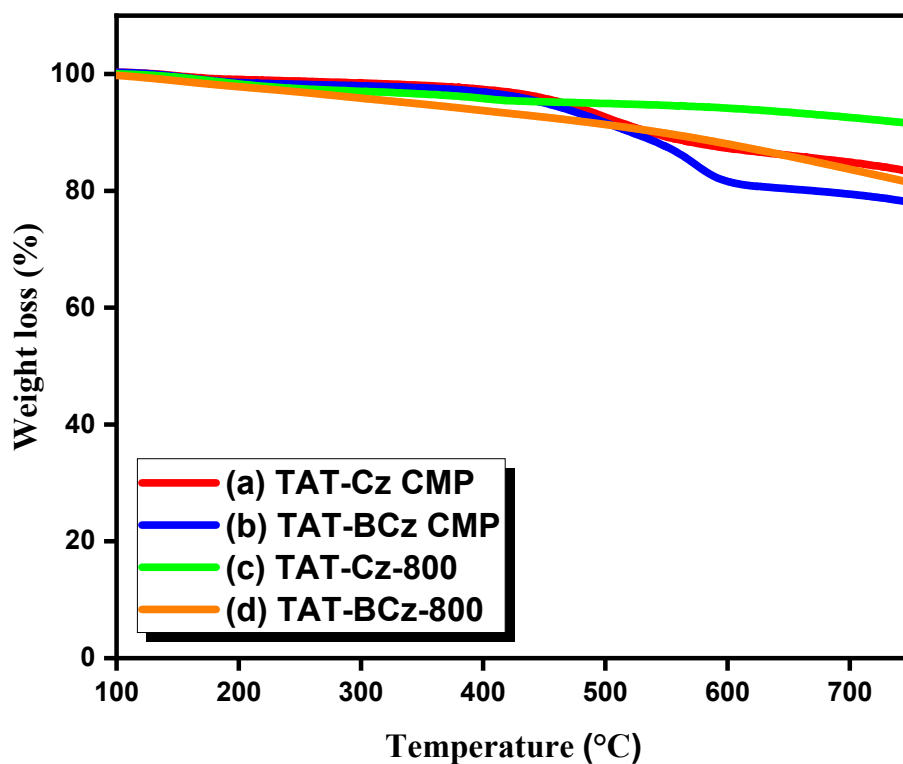


Figure S12. TGA curves of (a) TAT-Cz CMP, (b) TAT-BCz CMP, (c) TAT-Cz-800, and (d) TAT-BCz-800.

Table S1. Values of $T_{d10\%}$ and Char yield of CMPs and their calcinated materials.

Material	$T_{d10\%}$ (°C)	Char yield (%)
TAT-Cz CMP	536 °C	81 %
TAT-BCz CMP	521 °C	76 %
TAT-Cz-800	791 °C	90 %
TAT-BCz-800	545 °C	79 %

S8. X-ray Photoelectron Spectroscopy Analysis

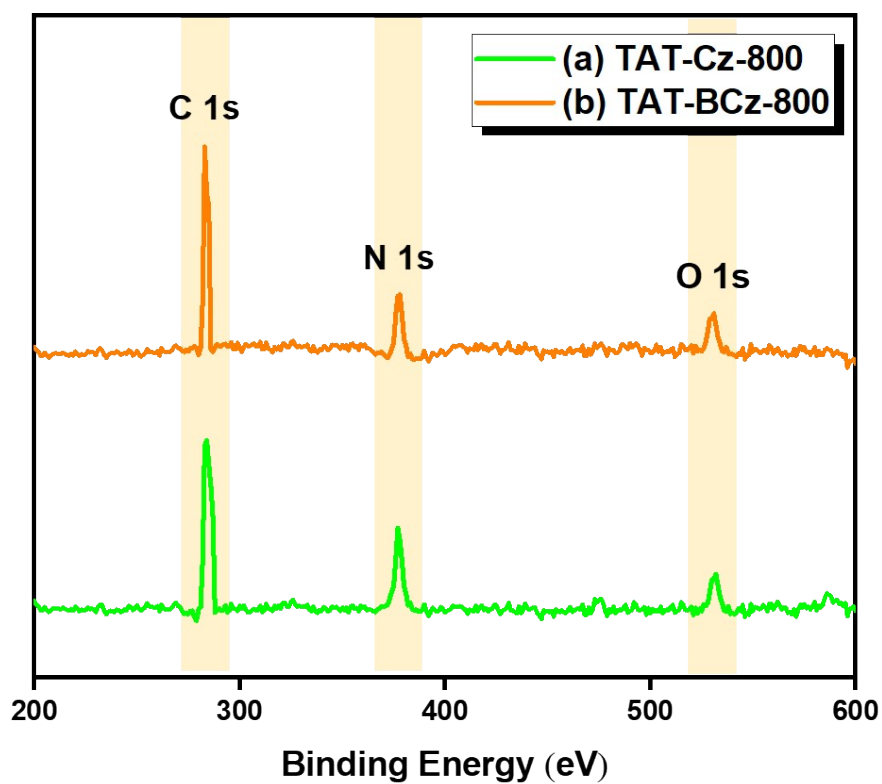


Figure S13. XPS spectra of (a) TAT-Cz-800, and (b) TAT-BCz-800.

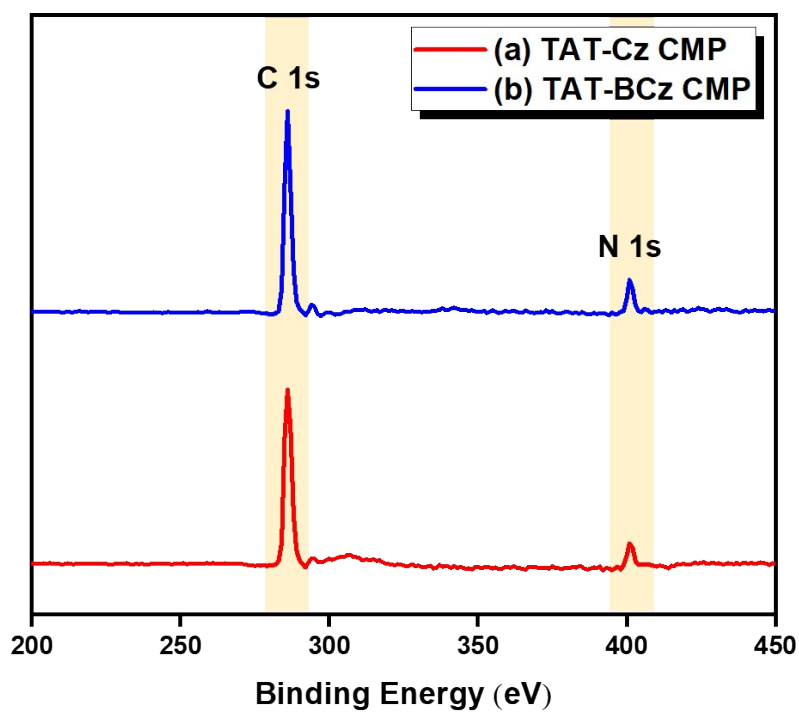


Figure S14. XPS spectra of (a) TAT-Cz CMP, and (b) TAT-BCz CMP.

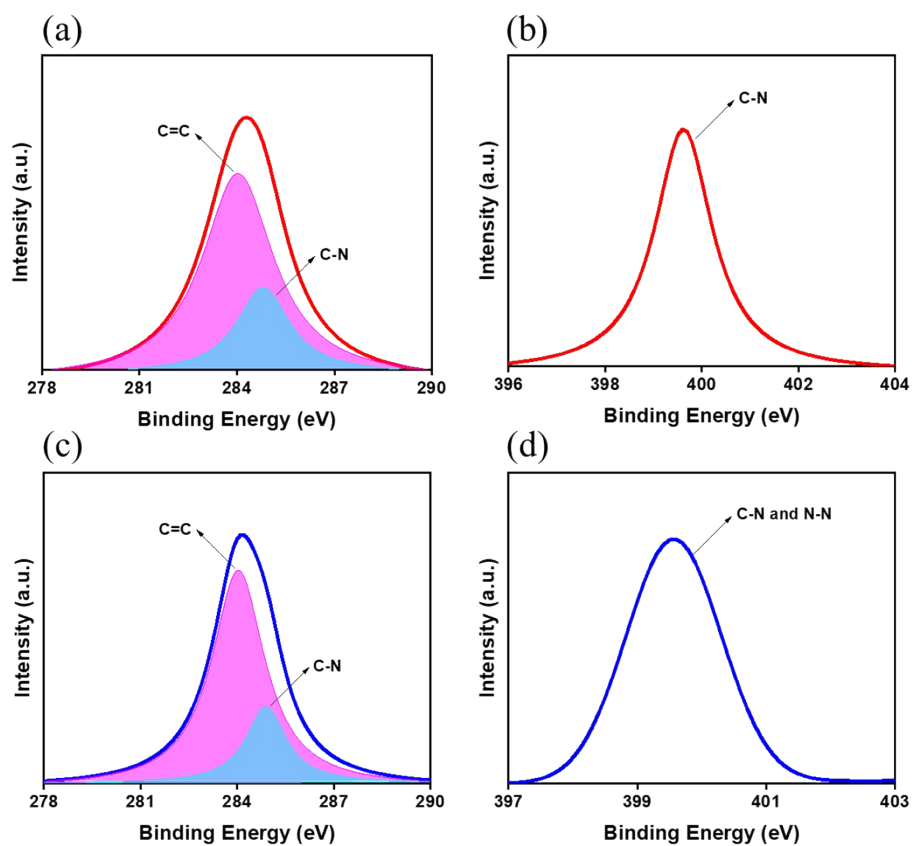


Figure S15. XPS analysis of (a) C1s peak, and (b) N1s peak of TAT-Cz CMP; (c) C1s peak, and (d) N1s peak of TAT-BCz CMP.

Table S2. XPS elemental analysis of TAT-Cz, TAT-BCz CMPs and their carbons.

Materials	%C	%N	%O
TAT-Cz CMP	79.25	14.42	---
TAT-BCz CMP	81.07	15.33	---
TAT-Cz-800	80.23	11.06	8.71
TAT-BCz-800	83.57	8.45	7.98

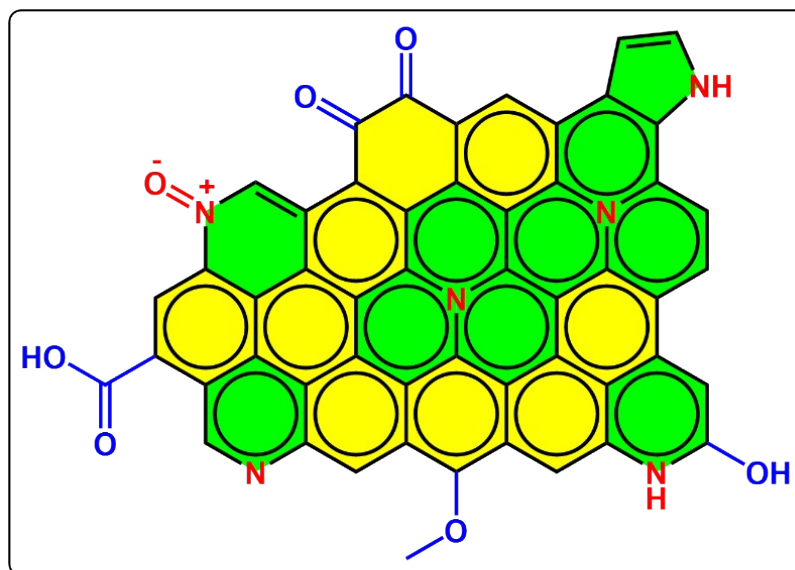
Table S3. Fitting data of XPS signals of TAT-Cz-800 and TAT-BCz-800 carbons.

CMPs	C species (%)			N species (%)				O species (%)		
	C=C	C=N	C=O	N-pyridine	N-pyrrole	N-quaternary	N-oxidized	O-quinone	O-ether	O-carboxylic
TAT-Cz-800	69.1	20.5	10.4	32.5	42.2	12.6	12.7	39.3	18.7	42.0
TAT-BCz-800	72.8	19.1	8.1	28.7	38.9	19.8	12.6	38.8	23.6	37.6

Table S4. Fitting data of XPS signals of TAT-Cz and TAT-BCz CMPs.

CMPs	C species (%)		N species (%)
	C=C	C-N	C-N/N-N
TAT-Cz	75.72	24.28	100
TAT-BCz	78.64	21.36	100

S9. The Proposed Chemical Structure of Carbon Materials



Microporous carbons

Figure S16. The proposed chemical structure of the produced carbon materials.

S10. X-ray Diffraction Analysis

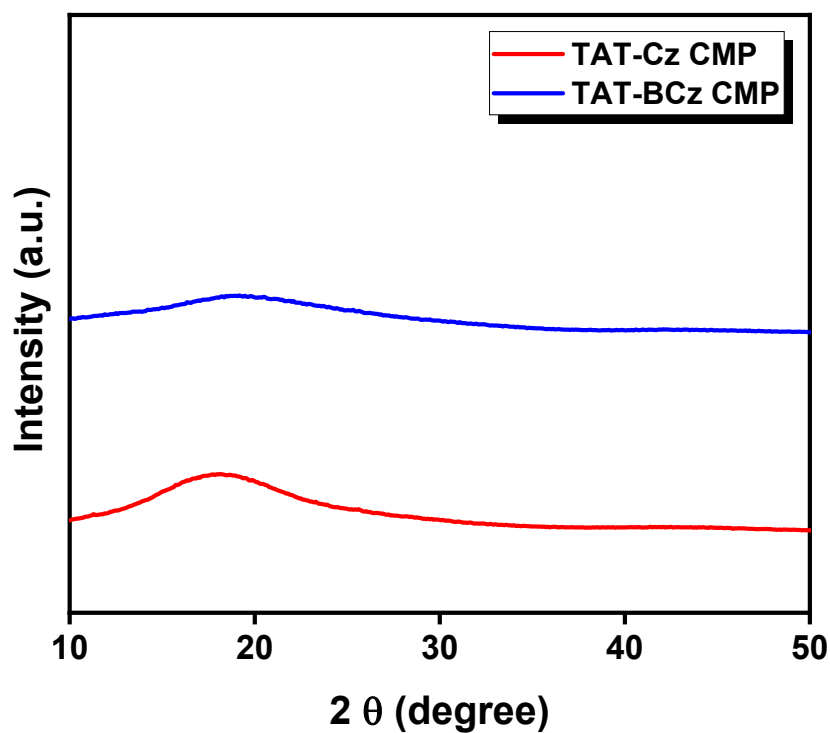


Figure S17. XRD analysis of the TAT-Cz and TAT-BCz CMPs.

S11. Raman Spectroscopy

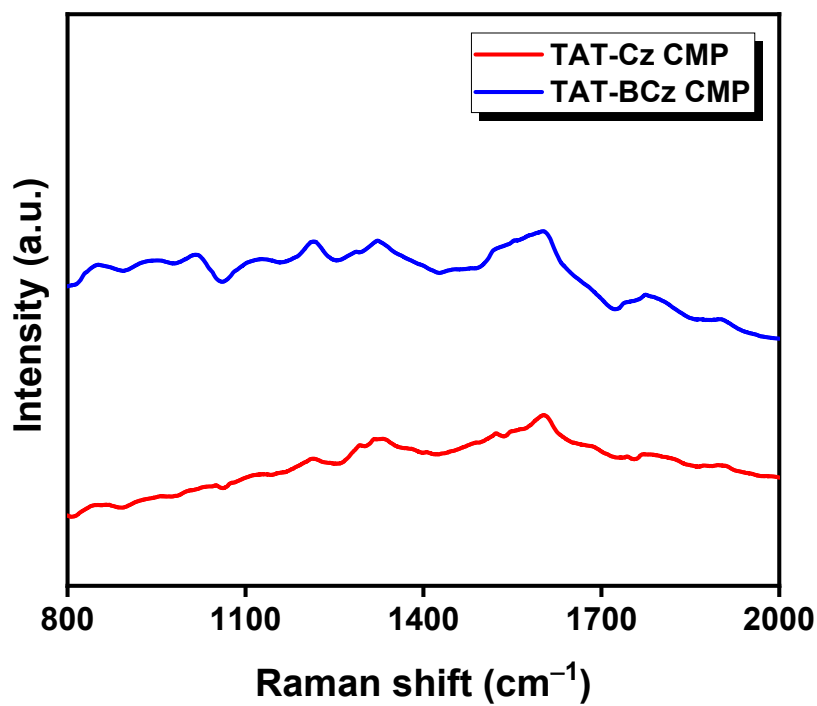


Figure S18. Raman spectra of the TAT-Cz and TAT-BCz CMPs.

S12. Elemental Analysis

Table S5. Elemental analysis of TAT-Cz CMP, TAT-BCz CMP, and their carbons.

No.	Sample name	Weight (mg)	Area CO ₂	Atom C (mg)	TC (Wt%)	Area N ₂	Atom N ₂ (mg)	TN (Wt%)
1	TAT-Cz CMP	1.56	3803922	0.94	81.45	73250	0.05	11.01
2	TAT-BCz CMP	1.31	1770142	0.45	82.17	146120	0.08	13.51
3	TAT-Cz-800	1.13	3571666	0.88	78.18	102993	0.06	13.22
4	TAT-BCz-800	1.10	3830939	0.95	86.36	146126	0.09	8.29

S13. Surface Area Parameters

Table S6. BET parameters of the synthesized CMPs and their corresponding carbons.

Material	S _{BET} (m ² g ⁻¹)	Pore size (nm)	Pore volume (cm ³ g ⁻¹)
TAT-Cz CMP	485	0.96	0.36
TAT-BCz CMP	128	1.03	0.09
TAT-Cz-800	600	1.07	0.75
TAT-BCz-800	384	1.80	0.16

S14. Low Magnification HR-TEM Spectroscopy

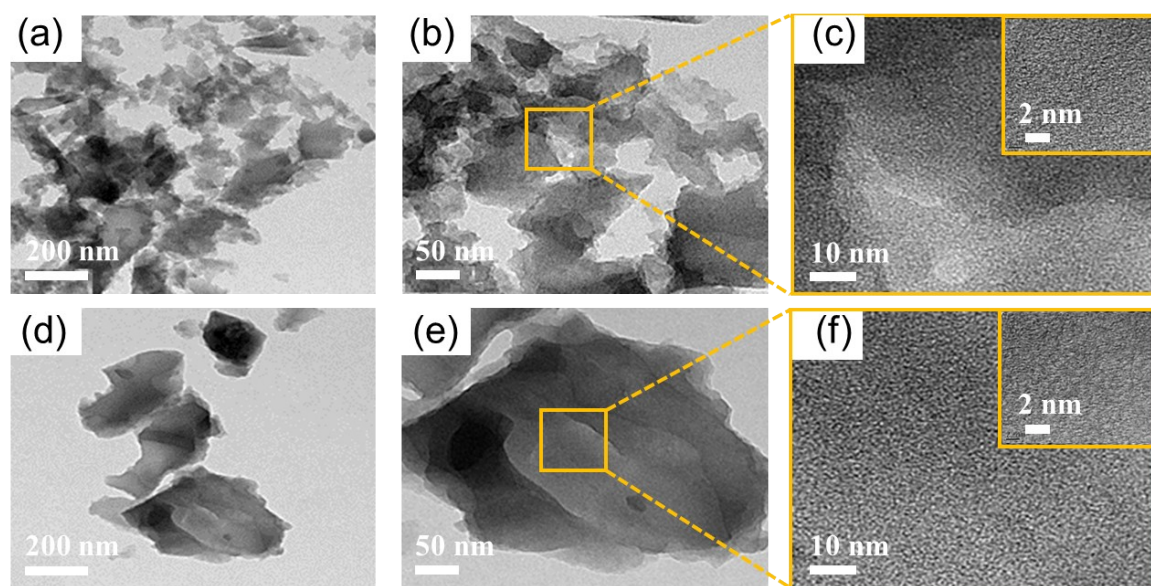


Figure S19. Low magnification HR-TEM photos (a-c) for TAT-Cz-800, and (d-f) for TAT-BCz-800 carbon materials.

S15. Contact Angle

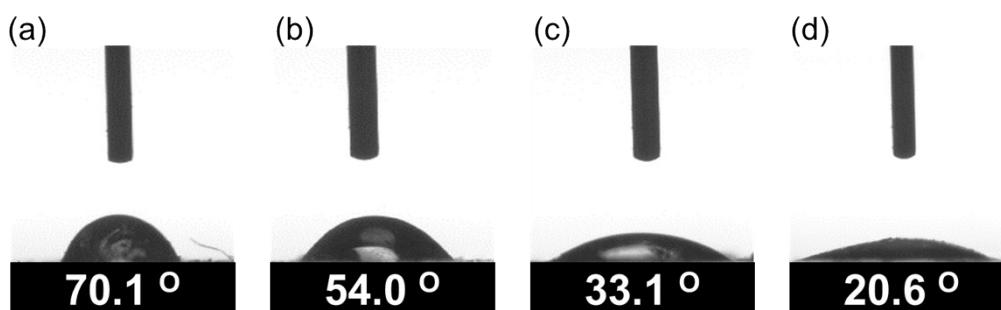


Figure S20. Water contact angle measurements for (a) TAT-Cz CMP, (b) TAT-BCz CMP, (c) TAT-BCz-800, and (d) TAT-Cz-800.

S16. Electrochemical Methods and Data

Working Electrode Cleaning: Prior to use, the glassy carbon electrode (GCE) was polished several times with 0.05- μm alumina powder, washed with EtOH after each polishing step, cleaned via sonication (5 min) in a water bath, washed with EtOH, and then dried in air.

Electrochemical Characterization: The electrochemical experiments were performed in a three-electrode cell using an Autolab potentiostat (PGSTAT204) and 1 M KOH as the aqueous electrolyte. The GCE was used as the working electrode (diameter: 5.61 mm; 0.2475 cm²). A Pt wire was used as the counter electrode; Hg/HgO (RE-61AP, BAS) was used as the reference electrode. All reported potentials refer to the Hg/HgO potential. The GCE was modified with CMP slurries, as described elsewhere, but with some modifications. [S7–S9] The slurries were prepared by dispersing the CMP (45 wt. %), carbon black (45 wt. %), and Nafion (10 wt. %) in EtOH (2 mL) and then sonicating for 1 h. A portion of this slurry (10 μL) was pipetted onto the tip of the electrode, which was then dried in air for 30 min prior to use. The electrochemical performance was studied through CV at various sweep rates (from 5 to 200 mV s⁻¹) and through the GCD method in the potential range from 0.0 to -1.0 V vs. Hg/HgO at various current densities (from 0.5 to 20 A g⁻¹) in 1 M KOH as the aqueous electrolyte solution. The specific capacitance was calculated from the GCD data using the following equation: [S9,S10]

$$C_s = (I\Delta t)/(m\Delta V) \quad [S11]$$

where C_s (F g⁻¹) is specific capacitance of the supercapacitor, I (A) is the discharge current, ΔV (V) is the potential window, Δt (s) is the discharge time, and m (g) is the mass of the CMP on the electrode. The energy density (E , Wh kg⁻¹), and the power density (P , W kg⁻¹) were calculated using the following equations: [S12]

$$E = 1000C(\Delta V)^2 / (2 \cdot 3600) \quad [S13]$$

$$P = E / (t/3600) \quad [S14]$$

We evaluated the electrochemical functionality of a symmetric supercapacitor using a CR2032 coin cell, which consists of an anode and cathode, a bottom and top cover, a metal spring, a separator, and an electrolyte. Our compounds served as both the cathode and the anode in order to construct a symmetric supercapacitor. The slurry was created by combining 2 mg of CMP, 2 mg of conductive carbon, 20 mL of Nafion, 200 mL of ethanol, and 400 mL of water. It was

then sonicated for an hour and cast onto carbon paper. We used a Selemion AMV membrane with an electrolyte of 1.0 M aqueous KOH.

The specific capacitance was calculated in assembled supercapacitor from the GCD data using the following equations:

$$C_s = 2(I\Delta t)/(m\Delta V)$$

where C_s ($F\ g^{-1}$) is the specific capacitance of the supercapacitor, I (A) is the discharge current, ΔV (V) is the potential window, Δt (s) is the discharge time, and m (g) is the mass of the CMP in the single electrode.

The energy density (E , $W\ h\ kg^{-1}$) and power density (P , $W\ kg^{-1}$) were calculated using the equations:

$$E_{cell} = 1000 C_s (\Delta V)^2 / (4 \cdot 2 \cdot 3600)$$

and

$$P_{cell} = E_{cell} / (t/3600)$$

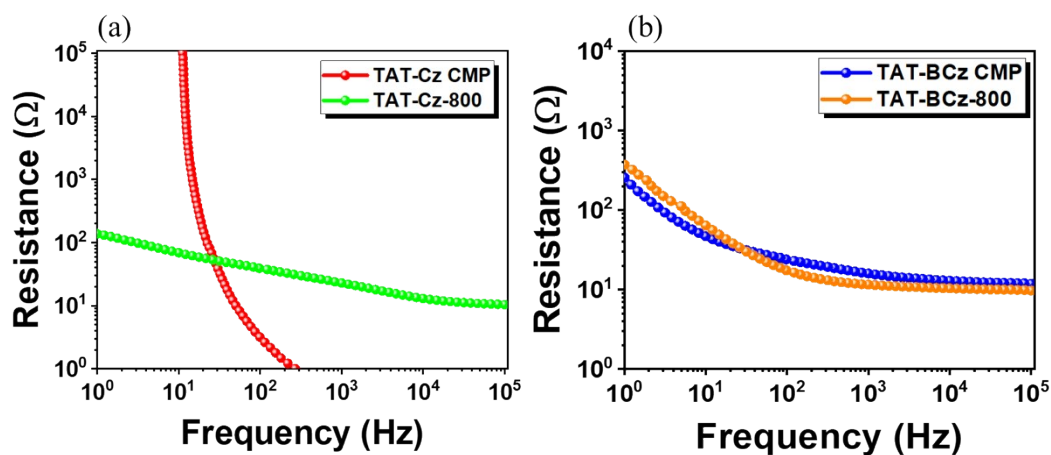


Figure S21. Bode plots of frequency with respect to resistance magnitude of (a) TAT-Cz CMP and TAT-Cz-800; (b) TAT-BCz CMP and TAT-BCz-800.

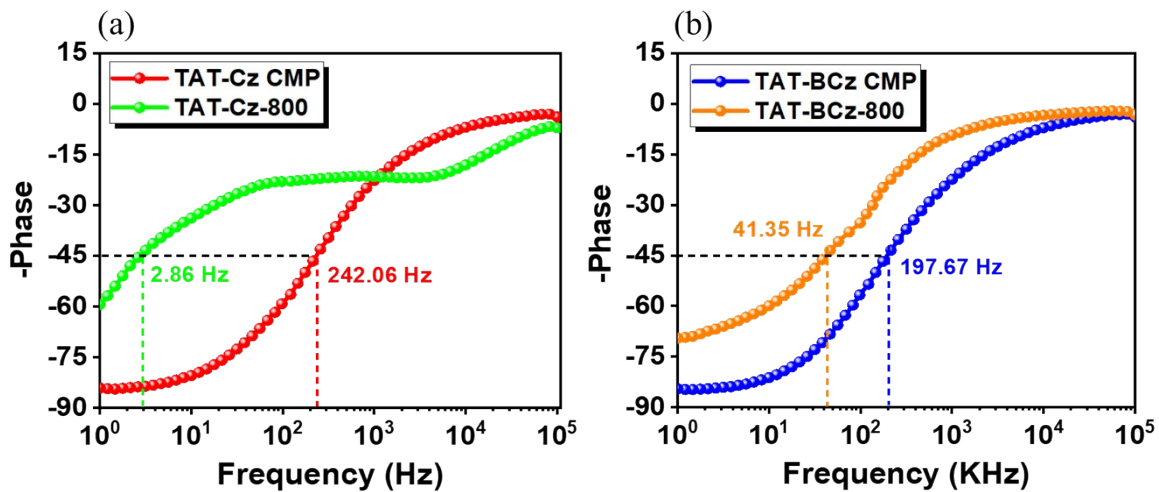


Figure S22. Bode plots of frequency with respect to phase angle to determine the knee frequency of polymers and their corresponding carbon materials in the three electrodes system.

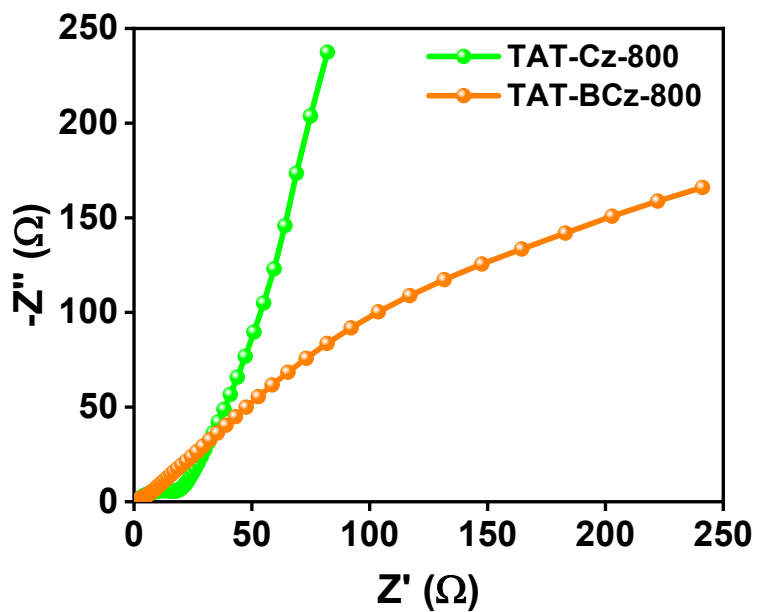


Figure S23. Nyquist plots of cells holding carbon materials in the two electrodes system.

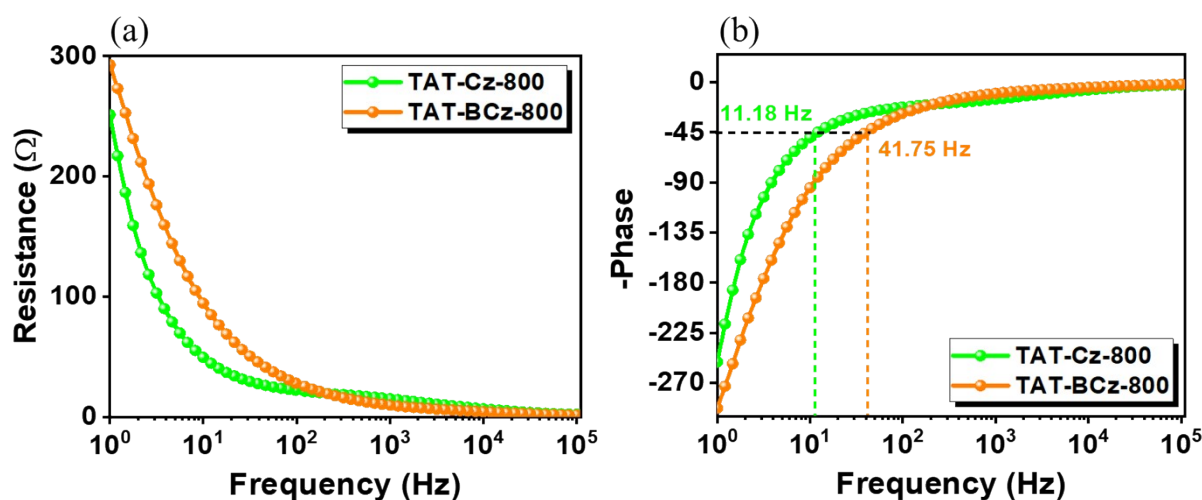


Figure S24. (a) Bode plots of frequency with respect to resistance magnitude. (b) Bode plots of frequency with respect to phase angle to determine the knee frequency of the carbon materials in the two electrodes system.

Table S7. Comparison between the specific surface area and specific capacitance of the synthesized TAT-based microporous carbons with those of previously reported materials for supercapacitor application.

Materials	S_{BET} ($\text{m}^2 \text{g}^{-1}$)	Capacitance	Ref.
Py-BDT	208	636 F g^{-1} at 0.5 A g^{-1}	<i>J. Mater. Chem. A</i> , 2023, 11, 19408–19417.
Py-Ph-BDT	427	712 F g^{-1} at 0.5 A g^{-1}	<i>J. Mater. Chem. A</i> , 2023, 11, 19408–19417.
MWCNT@SACMP-3	514	594 F g^{-1} at 1.0 A g^{-1}	<i>ACS Appl. Energy Mater.</i> 2022, 5, 3706–3714.
4KT-Tp COF	672	583 F g^{-1} at 0.2 A g^{-1}	<i>CCS Chemistry</i> , 2021, 3, 696–706.
PAQTA	331	576 F g^{-1} at 1.0 A g^{-1}	<i>Adv. Mater.</i> 2018, 30, 1705710.
Fc-CMPs/rGO	800	470 F g^{-1} at 0.5 A g^{-1}	<i>J. Mater. Chem. A</i> , 2018, 6, 18827–18832.
TCNQ	4000	383 F g^{-1} at 0.2 A g^{-1}	<i>Angew. Chem. Int. Ed.</i> 2018, 57, 7992–7996.
TPDA-1	545	348 F g^{-1} at 0.5 A g^{-1}	<i>ACS Sustain. Chem. Eng.</i> 2017, 6, 202–209.
PDC-MA	748	335 F g^{-1} at 1.0 A g^{-1}	<i>ACS Appl. Mater. Interfaces</i> 2019, 11, 26355–26363.

COF/rGO	246	269 F g ⁻¹ at 0.5 A g ⁻¹	<i>Nature Commun.</i> 2020, 11, 4712.
CAP-2	594	233 F g ⁻¹ at 1.0 A g ⁻¹	<i>ACS Nano.</i> 2018, 12, 852–860.
GH-CMP	219	206 F g ⁻¹ at 0.5 A g ⁻¹	<i>ChemElectroChem</i> 2019, 6, 5946–5950.
TAT-CMP-2	106	183 F g ⁻¹ at 1.0 A g ⁻¹	<i>Chem Sci.</i> 2017, 8, 2959–2965.
TAT-Cz-800	600	1005 F g⁻¹ at 1 A g⁻¹	This work
TAT-BCz-800	384	907 F g⁻¹ at 1 A g⁻¹	This work

S17. References

- [S1] M. R. Talipov, M. M. Hossain, A. Boddada, K. Thakura and R. Rathore, *Org. Biomol. Chem.*, 2016, **14**, 2961–2968.
- [S2] A. F. Saber, A. M. Elewa, H. H. Chou and A. F. M. EL-Mahdy, *Appl. Catal. B*, 2022, **316**, 121624.
- [S3] T. Xu, Y. Li, Z. Zhao, G. Xing and L. N. Chen, *Macromolecules*, 2019, **52**, 9786–9791.
- [S4] C. L. Chang, A. M. Elewa, J. H. Wang, H. H. Chou and A. F. M. EL-Mahdy, *Microporous Mesoporous Mater.*, 2022, **345**, 112258.
- [S5] K. Rakstys, A. Abate, M. I. Dar, P. Gao, V. Jankauskas, G. Jacopin, E. Kamarauskas, S. Kazim, S. Ahmad, M. Grätzel and M. K. Nazeeruddin, *J. Am. Chem. Soc.*, 2015, **137**, 16172–16178.
- [S6] T. Techajaronjit, S. Namuangruk, N. Prachumrak, V. Promarak, M. Sukwattanasinitt and P. Rashatasakhon, *RSC Adv.*, 2016, **6**, 56392.
- [S7] A. F. M. EL-Mahdy, Y. Hung, T. H. Mansoure, H. H. Yu, T. Chen and S. W. Kuo, *Chem. Asian J.*, 2019, **14**, 1429–1435.
- [S8] A. F. M. EL-Mahdy, C. Young, J. Kim, J. You, Y. Yamauchi and S. W. Kuo, *ACS Appl. Mater. Interfaces*, 2019, **11**, 9343–9354.
- [S9] C. R. DeBlase, K. E. Silberstein, T. T. Truong, H. D. Abruña and W. R. Dichtel, *J. Am. Chem. Soc.*, 2013, **135**, 16821–16824.
- [S10] A. Alabadi, X. Yang, Z. Dong, Z. Li and B. Tan, *J. Mater. Chem. A*, 2014, **2**, 11697–11705.
- [S11] M. G. Rabbani, A. K. Sekizkardes, O. M. El-Kadri, B. R. Kaafarani and H. M. El-Kaderi, *J. Mater. Chem.*, 2012, **22**, 25409–25417.
- [S12] L. Weijun, Z. Yixuan, Z. Jianyong, H. Jiajun, C. Zhenguang, M. W. Philip, C. Liuping and S. C. Yong, *Chem. Commun.*, 2014, **50**, 11942–11945.
- [S13] P. Rios, T. S. Carter, T. J. Mooibroek, M. P. Crump, M. Lisbjerg, M. Pittelkow, N. T. Supekar, G. J. Boons and A. P. Davis, *Angew. Chem. Int. Ed.*, 2016, **55**, 3387–3392.
- [S14] X. Yunfeng, C. Dan, F. Shi, Z. Chong and J. J. Xing, *New J. Chem.*, 2016, **40**, 9415–9423.